trans effect of triethylphosphine (**4B**) greater than that of chloride (**4A**) and possibly an additional cis effect for the extra triethylphosphine in **7**. Relative to the closely related $[PtCl(PEt_3)\{C(P(S)Ph_2)_3\text{-}S,S\}]$,[29] where exchange of two P=S groups occurs by rotation about a Pt–S bond with an activation energy of 67 kJ mol^{-1}, the exchange in **4B** is facilitated by the proximity of the P=S group. Examination of the two solid-state structures[13,29] shows that the exchange process in the tris(phosphine sulfide) complex requires more structural reorganization.

Acknowledgment. We thank the Natural Sciences and Engineering Research Council of Canada and the University of Victoria for research grants and Mrs. C. Greenwood for recording NMR spectra.

Contribution from the Department of Chemistry,
Texas A&M University, College Station, Texas 77843

Stereochemical Nonrigidity in Heterobimetallic Complexes Containing the Bent Metallocene–Thiolate Fragment

Marcetta Y. Darensbourg,* Magdalena Pala, Stephen A. Houliston, K. Paul Kidwell, David Spencer, Stephen S. Chojnacki, and Joseph H. Reibenspies

Received June 16, 1991

The physical properties and reactions of $Cp_2Ti(S\text{-}p\text{-}C_6H_4X)_2$ (**1**) and $Cp_2Ti(\mu\text{-}S\text{-}p\text{-}C_6H_4X)_2Mo(CO)_4$ (**2**) (X = Cl, H, CH_3, OCH_3) complexes as well as the mechanism of the Cp site equilibration process in bimetallic complexes were investigated. Cyclic voltammographs recorded in CH_2Cl_2 showed two reversible waves for Ti(IV) ⇄ Ti(III) and Mo(0) ⇄ Mo(I) processes in **2** and one reversible wave for Ti(IV) ⇄ Ti(III) in **1**. Positions of these waves varied uniformly with the Hammett σ parameter of the X substituent. Variable-temperature ^{1}H NMR studies provided values for $\Delta G^{\ddagger}$ of the Cp equilibration process which are ca. 30 kJ/mol smaller than $\Delta G^{\ddagger}$ for $Cp_2Ti(S\text{-}p\text{-}C_6H_4X)_2$ displacement from **2** by CO. This indicates that the fluxional process in **2** does not occur through a ligand dissociation process and argues for a mechanism of pyramidal inversion on sulfur. The X-ray structure for $Cp_2Ti(\mu\text{-}S\text{-}p\text{-}C_6H_4Cl)_2Mo(CO)_4$ (**2a**) is reported. Complex **2a** crystallizes in the monoclinic space group $P2_1/n$, with a = 12.396 (7) Å, b = 16.78 (2) Å, c = 12.838 (9) Å, β = 94.29 (5)°, Z = 4, and V = 2662 (3) Å^3. The Ti atom is in pseudotetrahedral coordination environment whereas the Mo is octahedrally coordinated. The S1–Ti–S2 and S1–Mo–S2 angles are obtuse (100.8 (1) and 97.6 (1)°, respectively) and Ti–S–Mo angles are acute (80.8 (1)°) in the planar Ti–S_2–Mo ring, supportive of metal-metal interactions implied by spectroscopic and electrochemical data. The phenyl groups are in an anti arrangement with respect to the Ti–S_2–Mo plane.

Introduction

The conformations of bent metallocene–thiolate complexes, $Cp_2M(SR)_2$, and their heterobimetallic analogues, $Cp_2M(\mu\text{-}SR)_2M'L_n$, are attractive subjects for structure/bonding arguments.[1] Solid-state and theoretical studies of the mononuclear metal complexes find the orientation of the SR ligands relative to the Cp rings to be coupled to the S–M–S angle.[1e,f,2,3] That is, maximization of sulfur π-donor interactions with the metal in d^0 and light metal d^1 complexes leads to wide (94–100°) S–M–S angles and, as well, orients the SR groups in the endo(anti) configuration. [Interestingly the endo(syn) configuration (with both R groups on the same side of the MS_2 plane) has never been observed for mononuclear complexes, although several examples of this configuration are known in binuclear compounds; vide infra.] Acute S–M–S angles (72–85°) suggestive of severe repulsion between the electrons in the metal-based $1a_1$ HOMO and the M–S bonded pair[3] are found in d^2 complexes and most heavier metal d^1 complexes. Additionally, the sulfur lone-pair density is directed away from the filled or half-filled metal frontier orbitals, generating the exo configuration, and, as well, projects sterically unhindered electron pair sites for further interaction with electrophiles.

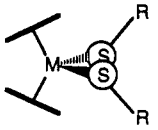

Endo(anti)

Exo

In fact, both configurational types of the bent metallocene–thiolates may be used as synthons for the formation of heterobimetallic complexes. The known orientations of thiolates in the bimetallics, endo(syn), endo(anti), and exo, may be rationalized by minor rotations of the SR ligand about the M–S bond of the monomer precursor to align sulfur lone pairs for bonding to an electron-deficient $M'L_n$ fragment (Figure 1). This leads to a puckered MS_2M' core for the exo precursors and a planar MS_2M' core for the endo precursors. Solid-state structures of binuclear complexes derived from precursors of the endo(anti) configuration have been observed to either have sulfur-bound groups on the same side of the MS_2M' plane in the endo(syn) conformation or on opposite sides of the MS_2M' plane in an endo(anti) conformation. Although we have represented the endo(syn) monomer as precursor to the endo(syn) bimetallic in Figure 1, there is no requirement that rearrangement to this (evidently) less favored configuration occurs prior to binding to M'. These bimetallics are fluxional, and in fact, the structural interconversion between bimetallic endo(anti) and endo(syn) is a focus of this work.

Several of the heterobimetallics derived from d^0 bent metallocene–thiolates have been noted to be stereochemically nonrigid in solution as evidenced by variable-temperature ^{1}H NMR spectra. The nonequivalent Cp ligands in the syn conformation have two resonances in the limit of slow exchange whereas a single resonance

(1) (a) Darensbourg, M. Y.; Silva, R.; Reibenspies, J.; Prout, C. K. *Organometallics* **1989**, *8*, 1315. (b) Muller, E. G.; Watkins, S. F.; Dahl, L. F. *J. Organomet. Chem.* **1976**, *111*, 73. (c) Wark, T. A.; Stephan, D. W. *Organometallics* **1989**, *8*, 2836. (d) Carrondo, M. A. A. F. d. C. T.; Jeffrey, G. A. *Acta Crystallogr.* **1983**, *C39*, 42. (e) Carrondo, M. A. A. F. d. C. T.; Matias, P. M.; Jeffrey, G. A. *Acta Crystallogr.* **1984**, *C40*, 932. (f) Calhorda, M. J.; Carrondo, M. A. A. F. d. C. T.; Dias, A. R.; Frazao, C. F.; Hursthouse, M. B.; Simoes, J. A. M.; Teixeira, C. *Inorg. Chem.* **1988**, *27*, 2513. (g) Davies, G. R.; Kilbourn, B. T. *J. Chem. Soc. A* **1971**, 87. (h) Kopf, H.; Rathlein, K. H. *Angew. Chem., Int. Ed. Engl.* **1969**, *8*, 980. (i) Braterman, P. S.; Wilson, V. A.; Joshi, K. K. *J. Chem. Soc. A* **1971**, 191. (j) Cameron, T. S.; Prout, K. C.; Rees, G. V.; Green, M. L. H.; Joshi, K. K.; Davies, G. R.; Kilbourn, B. T.; Braterman, P. S.; Wilson, V. A. *J. Chem. Soc., Chem. Commun.* **1971**, 14. (k) Braterman, P. S.; Wilson, V. A.; Joshi, K. K. *J. Organomet. Chem.* **1971**, *31*, 123. (l) Joshi, K. K.; Wardle, R.; Wilson, V. A. *Inorg. Nucl. Chem. Lett.* **1970**, *6*, 49. (m) Kotz, J. C.; Vining, W.; Coco, W.; Rosen, R.; Dias, A. R.; Garcia, M. H. *Organometallics* **1983**, *2*, 68. (n) Cameron, T. S.; Prout, K. C. *Chem. Commun.* **1971**, 161. (o) Wark, T. A.; Stephan, D. W. *Inorg. Chem.* **1987**, *26*, 363. (p) Ruffing, C. J.; Rauchfuss, T. B. *Organometallics* **1985**, *4*, 524. (q) Ashby, M. T. *Comments Inorg. Chem.* **1990**, *10*, 297.
(2) Darensbourg, M. Y.; Bischoff, C. J.; Houliston, S. A.; Pala, M.; Reibenspies, J. *J. Am. Chem. Soc.* **1990**, *112*, 6905.
(3) Lauher, J. W.; Hoffmann, R. *J. Am. Chem. Soc.* **1976**, *98*, 1729.

0020-1669/92/1331-1487$03.00/0

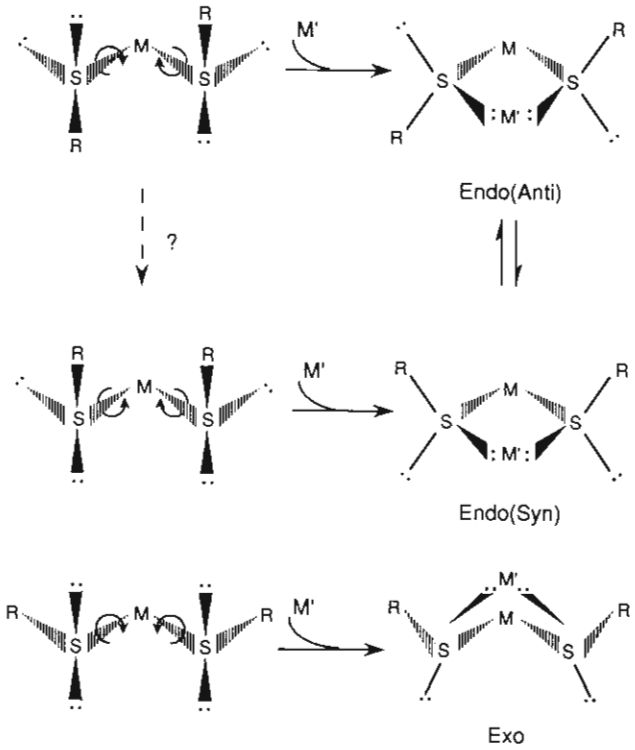

Figure 1. Rotations around the M–S bond which align sulfur lone pairs to bind with M'.

Scheme I

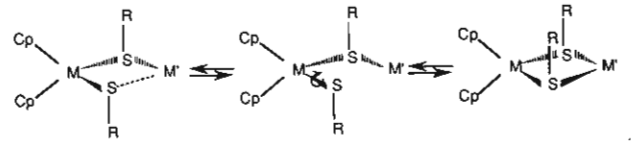

Scheme II

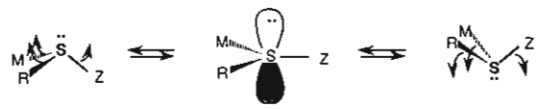

is found for the equivalent Cp ligands in the anti configuration. For a good number of $Cp_2M(\mu\text{-}SR)_2M'$ complexes, equilibrium studies find the two conformers to be of similar thermodynamic stabilities. For example endo(anti)/endo(syn) mixtures of $Cp_2Ti(\mu\text{-}SH)_2Mo(CO)_4$,[1p] $Cp_2Ti(\mu\text{-}SH)_2W(CO)_4$,[1p] $Cp_2Ti(\mu\text{-}SPh)_2Mo(CO)_4$,[1i] and $Cp_2Nb(\mu\text{-}SPh)_2Mo(CO)_4^+$ [1a] in the slow-exchange regime have K_{eq} values of 2, 1, 1, and 1.5, respectively. Upon warming of the solutions, the three signals for Cp coalesce into single peak in the fast-exchange limit.

Two possible mechanisms for Cp site equilibration in such complexes are depicted in Schemes I and II. A bond-breaking/rotation/bond re-formation process is expected to have activation parameters that would reflect the strength of the M'–S bond. Such a process has been proposed to be operative in $[Cp_2Ti(\mu\text{-}SEt)_2CuPR_3][PF_6]$ for which $\Delta G^{\ddagger}$ was determined from DNMR simulations of the VT ^1H NMR spectra to be 70–75 kJ/mol.[1o]

The other likely mechanism, pyramidal inversion at sulfur (Scheme II; Z = $M'L_m$ R), has been proposed for several fluxional processes and was recently reviewed.[4] Acute M–S–M' angles appear to impede pyramidal inversion processes. The inversion barrier also depends inversely on steric bulk of the substituents on sulfur as determined for the series $(RSCH_2CH_2SR)Mo(CO)_4$ ($\Delta G^{\ddagger}$ = 50.0, 46.6, 42.9, 40.2 kJ/mol, for R = Me, Et, ^{i}Pr, ^{t}Bu, respectively).[5a] Examples involving sulfur bound to two metals and one carbon have $\Delta G^{\ddagger}$ values that range from 30 to 70 kJ/mol.[1o,p,5b,c] Since the upper range values reported for pyramidal inversion are close to those purported for the bond-breaking processes, ambiguity in mechanistic interpretation results.

The heterobimetallics $Cp_2Ti(\mu\text{-}S\text{-}p\text{-}C_6H_4X)_2Mo(CO)_4$ offer the unique opportunity to definitively establish the mechanism of Cp site equilibration process and the effects of substituents on the energetics of that process. That is, the energetics of the S–Mo bond-breaking process may be probed through the reaction of $Cp_2Ti(\mu\text{-}S\text{-}p\text{-}C_6H_4X)_2Mo(CO)_4$ with CO to produce $Cp_2Ti(S\text{-}p\text{-}C_6H_4X)_2$ and $Mo(CO)_6$. Both the poor nucleophilicity of CO as well as the d^6 configuration of Mo^0 lend confidence that the displacement of the metallocene–thiolate by CO must procede through a dissociative, S_N1, mechanism.[6] A comparison of the activation data for this reaction for which Mo–S bond breaking governs the slow step and the activation data determined from the variable-temperature NMR spectra should establish whether the bond-breaking mechanism is a viable process for the change of configuration at sulfur in these complexes. The series of para-substituted arenethiolate ligands also permits exploration of electronic effects of the thiolate ligand on the physical properties and reactions of $Cp_2Ti(S\text{-}p\text{-}C_6H_4X)_2$ and the $Cp_2Ti(\mu\text{-}S\text{-}p\text{-}C_6H_4X)_2Mo(CO)_4$ (X = Cl, H, CH_3, OCH_3) bimetallics.

Experimental Section

Methods and Materials. Anaerobic techniques, i.e., an argon-filled drybox and double-manifold Schlenk line, were used for the syntheses of compounds and transfer of samples. All solvents were distilled prior to use from the appropriate drying agents and stored under nitrogen. Titanocene dichloride (Aldrich), para-substituted thiols (Aldrich), PPh_3 (Aldrich), ^{13}CO (Isotech), and CO (Liquid Carbonic) were used as received without further purification. Triethylamine (Aldrich), norbornadiene (Aldrich), and spectrophotometric grade heptane (Aldrich) were degassed and stored under nitrogen.

The NMR spectra were recorded in acetone-d_6 or toluene-d_8 on Varian Gemini 200, XL 200, and XL 200E instruments. Cyclic voltammographs were obtained using the Bioanalytical Systems 100A electrochemical analyzer and were recorded with a Pt metal working electrode, Pt wire auxiliary electrode, and Ag/AgCl reference electrode. Solutions (THF or CH_2Cl_2 as solvent) were 0.1 M in $[n\text{-}Bu_4N][PF_6]$ electrolyte and 0.001 M in solute. Electronic spectra were recorded on an IBM model 9420 UV–visible spectrophotometer. Infrared solution spectra were recorded on an IBM FT-IR Model 32 spectrophotometer. Kinetic measurements were performed on an IBM FT-IR Model 85 spectrophotometer equipped with an MCT detector. Elemental analyses were performed by Galbraith Laboratories, Knoxville, TN.

Synthesis of $C_7H_8Mo(CO)_4$. This procedure is a modification of several published methods.[7] To 7.65 g (28.4 mmol) of $Mo(CO)_6$ was added 150 mL of THF, and the solution was refluxed for 24 h. Next, 4 mL of degassed norbornadiene was added followed by another 4-mL aliquot 5 h later. The reaction mixture was refluxed for 40 h at a temperature not exceeding 90 °C. The solution was cooled to room temperature, the solvent removed under vacuum, and the residue extracted with 80 mL of hexane. The hexane extract was filtered through Celite to give a clear orange solution from which yellow crystals were obtained upon cooling. Concentrating the mother liquor gave a second crop of crystals. Total yield: 8.10 g, 95%. IR (ν(CO), THF): 2041 mw, 1949 s, 1893 m.

Syntheses of $Cp_2Ti(S\text{-}p\text{-}C_6H_4X)_2$ (X = OCH_3, CH_3, H, Cl). (This is a modification of the method reported by Giddings.[8]) To 40 mL of toluene was added 0.50 g (2.01 mmol) of titanocene dichloride, 4.02 mmol of the appropriate thiol, and 10 mL of triethylamine. The mixture was stirred for 30 min at room temperature and refluxed for 1 h. A color change from red to deep burgundy was observed after approximately 5

(4) Abel, E. W.; Bhargava, S. K.; Orrell, K. G. *Prog. Inorg. Chem.* **1984**, *32*, 1 and references therein.

(5) (a) Abel, E. W.; Budgen, D. E.; Moss, I.; Orrell, K. G.; Sik, V. *J. Organomet. Chem.* **1989**, *362*, 105. (b) Natile, G.; Maresca, L.; Bor, G. *Inorg. Chim. Acta* **1977**, *23*, 37. (c) Patel, V. D.; Boorman, P. M.; Kerr, K. A.; Moynihan, K. J. *Inorg. Chem.* **1982**, *21*, 1383.

(6) (a) Darensbourg, D. J. In *The Chemistry of Metal Cluster Complexes*; Shriver, D. F., Kaesz, H. D., Adams, R. D., Eds.; VCH: New York, 1990; Chapter 4. (b) Darensbourg, D. J. *Adv. Organomet. Chem.* **1982**, *21*, 113.

(7) (a) King, R. B.; Fronzagalia, A. *Chem. Commun.* **1966**, 274. (b) King, R. B.; Fronzagalia, A. *Chem. Commun.* **1965**, 547. (c) King, R. B.; Fronzagalia, A. *Inorg. Chem.* **1966**, *5*, 1837. (d) Werner, H.; Prinz, R. *Chem. Ber.* **1967**, *100*, 265.

(8) Giddings, S. A. *Inorg. Chem.* **1967**, *6*, 849.

min. The reaction mixture was filtered hot through Celite and the solvent removed in vacuo. The solid residue was recrystallized from 5 mL of THF/30 mL of pentane, and the resulting purple crystals were washed with three 10-mL portions of pentane. Yields were in the range 63–73%. Anal. Found (calc) for X = OCH_3: C, 63.13 (63.15); H, 5.31 (5.30). Found (calc) for X = CH_3: C, 67.49 (67.90); H, 5.80 (5.70). Found (calc) for X = Cl: C, 56.83 (56.78); H, 3.88 (3.90).

Syntheses of $Cp_2Ti(\mu\text{-}S\text{-}p\text{-}C_6H_4X)_2Mo(CO)_4$ (X = OCH_3, CH_3, H, Cl). Into a 50-mL Schlenk flask was placed 0.30 mg of the appropriate titanium compound, a 100% excess of $C_7H_8Mo(CO)_4$, and 15 mL of toluene. The solutions were stirred for 4–6 days, and a color change from burgundy to blue was observed after 30 min in all cases except for X = Cl. For this compound, the mixture changed color from red-purple to blue-purple only after slight heating. The solvent was removed from the reaction mixture in vacuo, and the residues were washed with three 10-mL portions of hexane to afford very dark blue powders. Yields for all derivatives were in the range of 76% (X = Cl) to 90% (X = H). Anal. Found (calc) for X = OCH_3: C, 51.05 (50.61); H, 3.43 (3.64). Found (calc) for X = Cl: C, 46.08 (46.38); H, 2.74 (2.69).

Reaction of $Cp_2Ti(\mu\text{-}S\text{-}p\text{-}C_6H_4OCH_3)_2Mo(CO)_4$ with PPh_3. A 50-mL Schlenk flask was loaded with 0.050 g (0.075 mmol) of $Cp_2Ti(\mu\text{-}S\text{-}p\text{-}C_6H_4OCH_3)_2Mo(CO)_4$, 0.050 g (0.191 mmol) of PPh_3, and 10 mL of toluene. The reaction mixture was stirred at room temperature for ~20 h. The color of the reaction mixture changed from blue to purple overnight. The *cis*-$(PPh_3)_2Mo(CO)_4$ complex was identified in the IR spectrum by comparison of ν(CO) of the reaction mixture with a standard. The solvent was removed from the reaction mixture and the residue washed (2 × 10 mL) with hexane. The remaining purple solid was dissolved in acetone-d_6 and identified as $Cp_2Ti(S\text{-}p\text{-}C_6H_4OCH_3)_2$ from the ^1H NMR spectrum.

Reaction of $Cp_2Ti(\mu\text{-}S\text{-}p\text{-}C_6H_4OCH_3)_2Mo(CO)_4$ with ^{13}CO. A 50-mL Schlenk flask was loaded with 0.057 g (0.086 mmol) of $Cp_2Ti(\mu\text{-}S\text{-}p\text{-}C_6H_4OCH_3)_2Mo(CO)_4$ and 5 mL of toluene and then cooled in dry ice. The flask was evacuated, back-filled with ^{13}CO, and stirred for 77 h. As ν(CO) corresponding to the starting material disappeared, frequencies corresponding to *cis*-$(^{13}CO)_2Mo(CO)_4$ appeared at 2005, 1984, 1957, and 1912 cm^{-1}.

Kinetics for the Reaction of $Cp_2Ti(\mu\text{-}S\text{-}p\text{-}C_6H_4X)_2Mo(CO)_4$ with CO (X = OCH_3, Cl). The kinetic measurements were carried out in a modified Parr minireactor containing an embedded Si cylindrical internal reflectance (CIR) crystal, a magnetically driven impeller stirring system, a T-type thermocouple, and a heating unit.[9] Temperature control was accomplished using a Parr temperature and stirring controller. In a typical run, 90–110 mg of $Cp_2Ti(\mu\text{-}S\text{-}p\text{-}C_6H_4X)_2Mo(CO)_4$ was placed in a vial, and 10 mL of toluene was added. The solution was drawn into the evacuated reactor and placed into the optical bench of the spectrophotometer. The system was then heated to the proper temperature and pressurized with CO. The reaction was monitored by following the disappearance of the ν(CO) stretching frequency at 1909 cm^{-1} (X = OCH_3) or 1913 cm^{-1} (X = Cl).

Variable-Temperature NMR Studies and DNMR Simulations. Variable-temperature ^1H NMR spectra of the complexes $Cp_2Ti(\mu\text{-}S\text{-}p\text{-}C_6H_4X)_2Mo(CO)_4$ were collected at 10 °C intervals. For each compound, coalescence of the Cp signals occurred within such a 10 °C range; thus, an average of the temperatures between which coalescence occurred was used to calculate ΔG^*. DNMR simulations for the VT NMR spectra of $Cp_2Ti(\mu\text{-}S\text{-}p\text{-}C_6H_4X)_2Mo(CO)_4$ were computed using standard line shape equations.[10] Simulations of the three site exchange were accomplished using the Kubo–Sack method.[11,12]

X-ray Structure Determination of $Cp_2Ti(\mu\text{-}S\text{-}p\text{-}C_6H_4Cl)_2Mo(CO)_4$. Collection and Reduction of X-ray Data. Preliminary examination and data collection were performed on a Nicolet R3m/V X-ray diffractometer[13] using Mo Kα (λ = 0.71073 Å) radiation and an oriented graphite crystal monochromator. The diameter of the collimated X-ray beam was 1.0 mm. X-ray diffraction quality crystals were obtained from a toluene solution layered with pentane. A dark red plate, 0.18 mm × 0.20 mm × 0.22 mm, was mounted on a glass fiber with epoxy cement and then cooled to 193 K in an N_2 cold stream. ω scans for several intense reflections indicated poor crystal quality. The cell lattice was determined to be monoclinic. Data were collected employing the θ–2θ scan type where $4.0° \le 2\theta \le 50.0°$. The scan range for the data collection was 1.20° plus the Kα separation with a variable scan rate of 1.50–14.65 deg/min. Three control reflections collected every 97 reflections showed no significant trends. Background measurements were obtained using stationary crystal and stationary counter techniques at the beginning and end of each scan for half of the total scan time. Lorentz and polarization corrections were applied to the data. A semiempirical absorption correction[14] was applied where T_{max} = 0.9887 and T_{min} = 0.8181.

Table I. Experimental Data for the X-ray Crystal Structure of $Cp_2Ti(\mu\text{-}S\text{-}p\text{-}C_6H_4Cl)_2Mo(CO)_4$

molecular formula	$C_{26}H_{18}Cl_2O_4S_2TiMo$
fw	673.3
space group	monoclinic, $P2_1/n$ (No. 14)
a, Å	12.396 (7)
b, Å	16.78 (2)
c, Å	12.838 (9)
β, deg	94.29 (5)
V, Å^3	2662 (3)
Z	4
ρ(calcd), g cm^{-3}	1.680
temp, K	193
radiation (λ, Å)	Mo Kα (0.71073)
abs coeff, mm^{-1}	1.141
min/max transm coeff	0.8181/0.9887
R, %[a]	5.82
R_w, %[a]	5.44

[a] Residuals: $R = \sum|F_o - F_c|/\sum F_o$; $R_w = [[\sum w(F_o - F_c)^2]/[\sum w \times (F_o)^2]]^{1/2}$.

Table II. Selected Data for $Cp_2Ti(\mu\text{-}S\text{-}p\text{-}C_6H_4Cl)_2Mo(CO)_4$

	Distances (Å)		
Ti–S1	2.477 (4)	Mo–S1	2.544 (3)
Ti–S2	2.486 (3)	Mo–S2	2.540 (3)
Cl1–C7	1.737 (9)	S1–C10	1.787 (8)
Cl2–C13	1.773 (8)	S2–C16	1.790 (8)
Ti···Mo	3.256 (3)	S1···S2	3.825
Mo–C1	2.045 (9)	C1–O1	1.132 (11)
Mo–C2	2.032 (9)	C2–O2	1.144 (11)
Mo–C3	1.973 (10)	C3–O3	1.164 (13)
Mo–C4	1.996 (9)	C4–O4	1.156 (11)
	Angles (deg)		
S1–Ti–S2	100.8 (1)	S1–Mo–S2	97.6 (1)
Ti–S1–Mo	80.8 (1)	Ti–S2–Mo	80.8 (1)
Ti–S1–C10	119.5 (3)	Ti–S2–C16	116.3 (3)
Mo–S1–C10	119.0 (3)	Mo–S2–C16	118.2 (3)
Cp–Ti–Cp	131.2		

Solution and Refinement. The molecular structure was solved by direct methods[15] and refined using a full-matrix least-squares method [quantity minimized $\sum w(F_o - F_c)^2$, where $w^{-1} = \sigma^2F + gF^2$]. All non-hydrogen atoms were refined anisotropically, and the hydrogen atoms were placed in idealized positions with the isotropic thermal motion fixed at 0.08. Refinement yielded R = 0.058, R_w = 0.054, and a goodness of fit = 1.74 at convergence. Neutral-atom scattering factors and anomalous scattering correction terms were taken from a standard source.[16] Experimental parameters are presented in Table I.

Results

Syntheses. All titanium complexes, $Cp_2Ti(S\text{-}p\text{-}C_6H_4X)_2$, were obtained by reaction of Cp_2TiCl_2 with HS-p-C_6H_4X (X = Cl, H, CH_3, OCH_3) in the presence of Et_3N. They are dark maroon solids which form air-sensitive solutions in toluene, benzene, THF, acetone, methylene chloride, and chloroform. The bimetallic complexes, $Cp_2Ti(\mu\text{-}S\text{-}p\text{-}C_6H_4X)_2Mo(CO)_4$, obtained for all from the displacement of norbornadiene (NBD) from $(NBD)Mo(CO)_4$, are deep blue in solution and as solids. Their solubilities are similar

(9) Darensbourg, D. J.; Gray, R. L.; Ovalles, C. *J. Mol. Catal.* **1987**, *41*, 329.
(10) Sandstrom, J. *Dynamic NMR Spectroscopy*; Academic: London, 1982; pp 12–15.
(11) (a) Lincoln, S. F. *Prog. React. Kinet.* **1977**, *9*, 1. (b) Johnson, C. S.; Moreland, C. G. *J. Chem. Educ.* **1973**, *50*, 477.
(12) DNMR program written by J. H. Horner.
(13) Diffractometer control software, P3VAX 3.42, supplied by Nicolet Analytical X-ray Instruments, Madison, WI.
(14) North, A. C. T.; Phillips, D.; Mathews, F. S. *Acta Crystallogr., Sect. A* **1968**, *24*, 351.
(15) All crystallographic calculations were performed with SHELXTL-PLUS rev 3.4 (G. M. Sheldrick, Institut fur Anorganische Chemie der Universitat, Tammannstrasse 4, D-3400, Gottingen, Federal Republic of Germany) supplied by Nicolet Analytical X-ray Instruments, Madison, WI.
(16) *International Tables for X-ray Crystallography*; Ibers, J. A., Hamilton, W. C., Eds.; Kynoch: Birmingham, England, 1974; Vol. 4, pp 99 and 149.

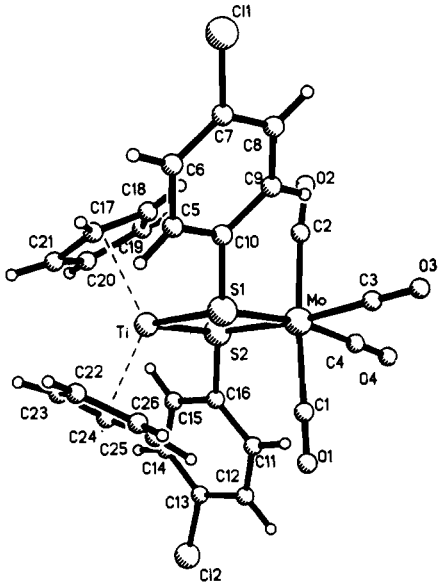

Figure 2. Molecular structure of $Cp_2Ti(\mu\text{-}S\text{-}p\text{-}C_6H_4Cl)_2Mo(CO)_4$ with complete numbering scheme.

to the titanium monomers, but they are much more air sensitive in solution. The solution stability of the heterobimetallics with respect to metallothiolate $[Cp_2Ti(S\text{-}p\text{-}C_6H_4X)_2]$ ligand loss depends both on solvent polarity and on the electron-donating ability of X. For example, in toluene evidence of disruption is seen only after several days for all bimetallics. In acetone solutions of $Cp_2Ti(\mu\text{-}S\text{-}p\text{-}C_6H_4CH_3)_2Mo(CO)_4$ the amount of monomeric $Cp_2Ti(S\text{-}p\text{-}C_6H_4CH_3)_2$ increased to 10% over a 48-h period whereas the $S\text{-}p\text{-}C_6H_4Cl$ analogue was 50% metallothiolate ligand dissociated at 24 h.

Characterization. The crystal structure was determined for $Cp_2Ti(\mu\text{-}S\text{-}p\text{-}C_6H_4Cl)_2Mo(CO)_4$ by X-ray diffraction techniques (Figure 2). Selected distances, bond lengths, and angles are listed in Table II. Complete listings of bond distances, bond angles, anisotropic displacement coefficients, H-atom coordinates, and structure factor tables are available as supplementary material.

Proton NMR spectra for both monometallic and bimetallic complexes were recorded in acetone-d_6 and toluene-d_8 (Table III). After coordination of $Cp_2Ti(S\text{-}p\text{-}C_6H_4X)_2$ to the $Mo(CO)_4$ center the signals of the aryl protons were shifted downfield, while the signals of Cp rings were shifted upfield (Table III). The Cp signals were also much broader than in the spectra of corresponding monomers.

Variable-temperature NMR spectra for $Cp_2Ti(\mu\text{-}S\text{-}p\text{-}C_6H_4X)_2Mo(CO)_4$ (Figure 3) were simulated by the DNMR program,[10-12] and activation parameters ($\Delta H^{\ddagger}$ and $\Delta S^{\ddagger}$) were obtained using the NLLSQ program[17] on an Apple IIE personal computer.

The electronic spectra for $Cp_2Ti(S\text{-}p\text{-}C_6H_4X)_2$ were recorded in THF solutions. They show an intense charge-transfer band below 340 nm and two well-separated peaks in the visible region (Table IV). The spectra for the bimetallics show an additional band that overlaps with that at ca. 540 nm; hence, the maxima values reported in Table IV are somewhat arbitrary. The bimetallic complexes were also characterized by IR spectroscopy (Table IV).

The cyclic voltammographs for all the compounds were recorded in THF. Those for the bimetallics were also taken in methylene chloride. Both the titanium monomers and Ti–Mo bimetallics show a single reversible wave for the reduction of titanium (Table IV and Figure 4). For the bimetallic complexes a second redox process is observed at about 980 mV and is attributed to the oxidation of molybdenum.

Reactions. The reactions of PPh_3 and ^{13}CO with $Cp_2Ti(\mu\text{-}S\text{-}p\text{-}C_6H_4X)_2Mo(CO)_4$ yielded the bent metallocene–thiolate, $Cp_2Ti(\mu\text{-}S\text{-}p\text{-}C_6H_4X)_2$, and *cis*-$L_2Mo(CO)_4$ as the only products. There was no evidence from IR spectra that ^{13}CO exchanged into the intact heterobimetallic.[18] Rates of reactions with CO were greatly accelerated in THF solutions (3 h to completion) as compared to reactions in toluene (3 days), and the same products were observed. The prolonged reaction times led to formation of an unidentified, non-CO- and non-Cp-containing titanium species as indicated by IR and NMR techniques.

(17) Christian, S. D.; Tucker, E. E. *Am. Lab.* **1982**, *14*, 36.

Table III. ^1H NMR Data (ppm) for $Cp_2Ti(S\text{-}p\text{-}C_6H_4X)_2$ and $Cp_2Ti(\mu\text{-}S\text{-}p\text{-}C_6H_4X)_2Mo(CO)_4$ Solutions at 22 ± 2 °C

			aryl			
X	solvent	Cp	X	H_s	H_x	J_{HH}, Hz
			$Cp_2Ti(S\text{-}p\text{-}C_6H_4X)_2$			
Cl	acetone	6.13		7.51	7.32	8.4
	toluene	5.57		7.49	7.05	8.7
H	acetone	6.10		(7.54 7.29 7.14)[a]		
CH_3	acetone	6.08	2.32	7.41	7.11	8.4
OCH_3	acetone	6.06	3.79	7.42	6.88	8.9
	toluene	5.70	3.34	7.69	6.74	8.9
			$Cp_2Ti(\mu\text{-}S\text{-}p\text{-}C_6H_4X)_2Mo(CO)_4$			
Cl	acetone	5.70		7.81	7.50	8.7
	toluene	4.87		7.39	*b*	8.8
H	acetone	5.68		(7.81 7.46 7.33)[a]		
	toluene	4.97		7.67[c]		
CH_3	acetone	5.66	2.36	7.67	7.27	8.2
	toluene	4.99	2.08	7.57	6.89	8.2
OCH_3	acetone	5.66	3.85	7.70	7.04	9.0
	toluene	5.02	3.27	7.58	6.71	8.9

[a] For a nonsubstituted ring the signals are listed in the order H_{ortho}, H_{meta}, and H_{para}. [b] Upper field doublet obscured by solvent signal. [c] Center of multiplet.

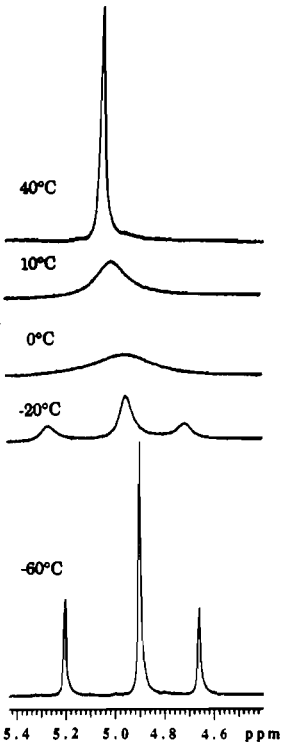

Figure 3. Variable-temperature ^1H NMR spectra of the Cp resonances in $Cp_2Ti(\mu\text{-}S\text{-}p\text{-}C_6H_4OCH_3)_2Mo(CO)_4$, in toluene-$d_8$.

Discussion

Structural Analysis. The molecular structure of $Cp_2Ti(\mu\text{-}S\text{-}p\text{-}C_6H_4Cl)_2Mo(CO)_4$ shows that Ti is in a pseudotetrahedral coordination environment with a Cp–Ti–Cp angle of 131.2° and a S–Ti–S angle of 100.8°. The Mo atom is octahedrally coor-

(18) Darensbourg, D. J.; Nelson, H. H., III; Murphy, M. A. *J. Am. Chem. Soc.* **1977**, *99*, 896.

Table IV. Electrochemical and Spectroscopic Results for $Cp_2Ti(S\text{-}p\text{-}C_6H_4X)_2$ and $Cp_2Ti(\mu\text{-}S\text{-}p\text{-}C_6H_4X)_2Mo(CO)_4$ Complexes in THF Solutions

	$Cp_2Ti(S\text{-}p\text{-}C_6H_4X)_2$		$Cp_2Ti(\mu\text{-}S\text{-}p\text{-}C_6H_4X)_2Mo(CO)_4$		
X	λ_{max}, nm	$E_{1/2}$, V	λ_{max}, nm[a]	ν(CO), cm^{-1}	$E_{1/2}$, V
Cl	398, 537	−1.028	*b*, 540, 590	2021 m, 1941 sh, 1928 sh, 1913 s, br	−0.589
H	399, 537	−1.129	390, 540, 595	2019 m, 1942 sh, 1924 sh, 1911 s, br	−0.640
CH_3	401, 540	−1.155	360, 540, 600	2018 m, 1943 sh, 1924 sh, 1910 s, br	−0.677
OCH_3	386, 420, 546	−1.186	380, 540, 608	2018 m, 1944 sh, 1921 sh, 1909 s, br	−0.706

[a] In toluene. [b] Shoulder on the intense charge-transfer band.

Table V. Variable-Temperature ^1H NMR Data[a] and CO-Substitution Data[b] for Bimetallic Complexes

	VT NMR				CO substitution		
X	T_c, K	$\Delta H^{\ddagger}$, kJ/mol	$\Delta S^{\ddagger}$, J/(mol·K)	$\Delta G^{\ddagger}$,[c] kJ/mol	$\Delta H^{\ddagger}$, kJ/mol	$\Delta S^{\ddagger}$, J/(mol·K)	$\Delta G^{\ddagger}$,[c] kJ/mol
Cl	258	46.6 ± 0.9	−16.1 ± 3.3	50.7 ± 1.7	88.2 ± 1.8	8.4 ± 5.8	86.0 ± 3.3
H	253	41.7 ± 3.0	−36.7 ± 11.6	51.0 ± 5.9			
CH_3	258	40.9 ± 1.7	−42.8 ± 6.6	51.9 ± 3.4			
OCH_3	268	59.1 ± 4.0	19.9 ± 15.1	53.8 ± 8.0	91.3 ± 1.2	21.0 ± 3.8	85.7 ± 2.2

[a] In toluene-d_8. [b] p_{CO} = 500 psi, temperature range 299–323 K, toluene solvent. [c] Calculated at T_c.

dinated, and the Ti–S_2–Mo ring is planar (the dihedral angle between the S1–Ti–S2 and S1–Mo–S2 planes is 0.90°). As expected, the Mo–CO distances trans to sulfur are apparently shorter than those for CO's trans to each other; however, the differences are statistically insignificant.

There is no crystal data available for the $Cp_2Ti(S\text{-}p\text{-}C_6H_4Cl)_2$ monomer; however, $Cp_2Ti(SC_6H_5)_2$[1b] and $Cp_2Nb(S\text{-}p\text{-}C_6H_4Cl)_2^+$[1a] are known. Both are of the endo configuration and have S–M–S angles of 99.4 and 102.3°, respectively. Hence, it would appear that utilizing the $Cp_2Ti(SAr)_2$ as a chelating ligand does little to the S–Ti–S angle. This is a result similar to that found for $Cp_2Nb(SPh)_2^+$ (∠S–Nb–S=101.4°) and $Cp_2Nb(\mu\text{-}SPh)_2Mo(CO)_4^+$ (∠S–Nb–S=101.8°).[1a]

The comparison of the structure reported here with that of $Cp_2Ti(\mu\text{-}SMe)_2Mo(CO)_4$[1g] shows no unusual differences in bond lengths or bond angles; the Ti···Mo distances are 3.256 (3) and 3.321 (2) Å, respectively, i.e., slightly shorter in the $\mu\text{-}S\text{-}p\text{-}C_6H_4Cl$ derivative. The two bimetallic complexes are definitely dissimilar in the arrangement of R groups on sulfurs with respect to the Ti–S_2–Mo plane. In the $Cp_2Ti(\mu\text{-}SMe)_2Mo(CO)_4$ complex both methyl groups are on the same side of Ti–S_2–Mo ring (the isomer referred to as endo(syn)), whereas in the $Cp_2Ti(\mu\text{-}S\text{-}p\text{-}C_6H_4Cl)_2Mo(CO)_4$ compound the phenyl rings are on the opposite sides of metal–sulfur plane. That is, the latter complex is another example of the endo(anti) configuration, similarly to the d^0 niobium(V) complex $[Cp_2Nb(\mu\text{-}SPh)_2Mo(CO)_4]^+$.[1a]

^1H NMR Spectra. At all temperatures (25 to −80 °C) a sharp signal for equivalent Cp's is present in the spectra of $Cp_2Ti(S\text{-}p\text{-}C_6H_4X)_2$ complexes. Two doublets are observed for the substituted aryl protons; the one more deshielded is assigned to those ortho to sulfur (H_S).[2] A similar pattern was observed in both acetone-d_6 and toluene-d_8; however, in the latter all signals are shifted upfield relative to the former. This phenomenon is not unusual and is known as aromatic solvent-induced shift (ASIS).[19,20]

Upon coordination of $Cp_2Ti(S\text{-}p\text{-}C_6H_4X)_2$ to the $Mo(CO)_4$ center to form $Cp_2Ti(\mu\text{-}S\text{-}p\text{-}C_6H_4X)_2Mo(CO)_4$, the signals of the aryl protons were shifted downfield (Table III), a consequence of the inductive effect of $Mo(CO)_4$. In contrast, the signals for the Cp rings were shifted *upfield*, indicating an increase of electron density on the Ti moiety. A similar effect was observed for the Cp chemical shifts in the $Cp_2Ti(SMe)_2$ and $Cp_2Ti(\mu\text{-}SMe)_2Mo(CO)_4$ complexes.[1h,i] The shielding was attributed to a Mo donor → Ti acceptor metal–metal interaction. As with the mononuclear bent metallocene–thiolate complexes, the same effects of para substituent and ASIS were observed.

Similar to $Cp_2Ti(SAr)_2$ monomers, a single signal for Cp ligands is seen in the NMR spectra of $Cp_2Ti(\mu\text{-}S\text{-}p\text{-}C_6H_4X)_2Mo(CO)_4$ at room temperature. However, this signal is much broader. Cooling the sample down to −60 °C leads to its separation into three signals that integrate approximately 1:2:1 (Figure 3). Upon warming of the solutions, the three peaks *simultaneously* broadened and coalesced into one signal, with a line width generally less than 2 Hz above 50 °C in toluene. The chemical shift corresponded to their weighted average, as expected. The Cp signals of all bimetallic complexes examined coalesced between 253 K (X = H) and 268 K (X = OCH_3). The values for activation parameters obtained from line shape analysis are listed in Table

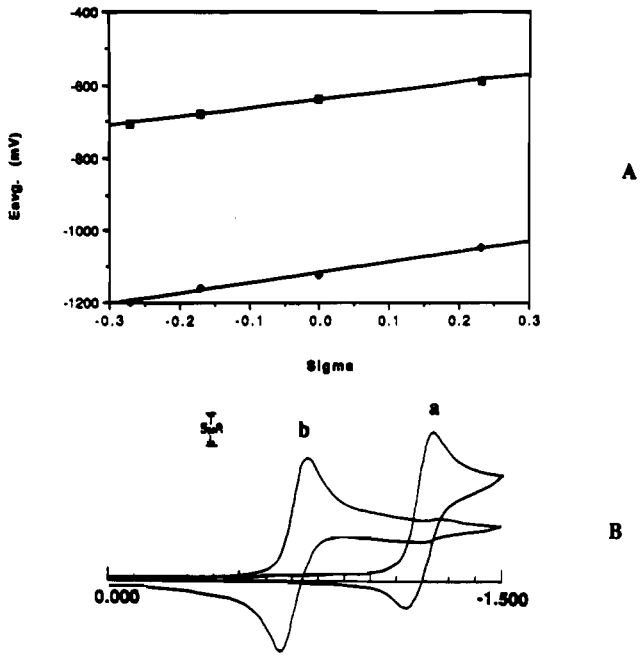

Figure 4. (A) Plots of Hammett σ constants for para substituents vs E_{av} values from cyclic voltammographs of $Cp_2Ti(S\text{-}p\text{-}C_6H_4X)_2$ and $Cp_2Ti(\mu\text{-}S\text{-}p\text{-}C_6H_4X)_2Mo(CO)_4$ in THF: ■, E_{av} (mV) for Ti(IV) → Ti(III) in bimetallic complexes; ◆, E_{av} (mV) for Ti(IV) → Ti(III) in monomeric complexes. (B) Cyclic voltammographs of monomeric (a) and bimetallic (b) complexes when X = OCH_3 (solvent THF; sweep rate 100 mV/s).

(19) Lambert, J. B.; Shurvell, H. F.; Verbit, L.; Cooks, R. G.; Stout, G. H. *Organic Structural Analysis*; Macmillan: Englewood Cliffs, NJ, 1976; p 44.

(20) The peculiarity of the solvent effect here is that in acetone-d_6 there is a very small, but consistent, upfield shift of the Cp signals with increasing electron-donating ability of X. In contrast, in toluene-d_8 the electronic influence of X on the Cp signal position is reversed. Since aromatic solvents are considered anisotropic, this may be due to solute–solvent interactions (e.g., π–π toluene–Cp interaction or charge transfer).

(21) Observed rate constants at 299 K for CO pressure: 100 psi, 1.04×10^{-4}; 200 psi, 1.25×10^{-4}; 300 psi, 1.61×10^{-4}; 500 psi, 1.46×10^{-4}; 660 psi, 1.41×10^{-4} s^{-1}. The CO solubility at 14.7 psi and 293 K in benzene and toluene is 7.32×10^{-3} and 7.49×10^{-3} mol L^{-1}, respectively. At 500 psi and 433 K the solubility in benzene is reported to increase dramatically to 0.328 mol L^{-1}.[22] A similar increase is expected for toluene, generating a minimum of 20–25-fold excess.

(22) Solubility Data Series; Pergamon: Oxford, New York, 1990; Vol. 43.

V. The $\Delta G^{\ddagger}$ values were calculated at coalescence temperature and, as noted in Table V, all are ca. 30 kJ/mol lower than those for the CO substitution process.

Electrochemistry. The cyclic voltammographs of the titanium monomers and Ti–Mo bimetallics both show a single reversible wave for the reduction of the titanium, i.e., Ti(IV) → Ti(III) process. As the para substituent on the *S*-aryl became more electron withdrawing, the reduction potentials became increasingly more positive, showing a linear correlation with the Hammett σ parameter (Figure 4).

The reduction potentials for all the heterobimetallics were approximately 480 mV more positive than their mononuclear titanocene–thiolate counterparts (Table IV and Figure 4), indicating that these complexes are more easily reduced. The facilitated addition of an electron to the bimetallic complex as compared to the mononuclear bent metallocene–thiolate is thought to result from increased electron delocalization in the bimetallic. The slopes for the σ vs E_{av} plots were nearly identical for both Ti monomers and heterobimetallics (Figure 4).

The bimetallic complexes undergo a second redox process, attributed to molybdenum oxidation.[1m] In THF the Mo(0) → Mo(I) process is irreversible and occurs at ca. 980 mV. In methylene chloride this oxidation is reversible and its potential decreases as the electron-donating ability of the para substituent increases; i.e., for X = Cl $E_{1/2}$ = 731 mV, for X = H $E_{1/2}$ = 692 mV, and for X = CH_3 $E_{1/2}$ = 662 mV.

Solvent-promoted disruption of the bimetallics was also evident in the cyclic voltammographs in THF by the buildup over time of the reversible wave at the value of the Ti(IV) → Ti(III) reduction for the monomer. It appears that this disruption process is mainly due to the polar donating solvent, since in methylene chloride no wave attributable to monomeric species was observed.

Electronic Spectra. The electronic spectra for $Cp_2Ti(S\text{-}p\text{-}C_6H_4X)_2$ are very similar to those reported by Braterman et al.[1i,j] They show an intense charge-transfer band below 340 nm and two well-separated peaks in the visible region (Table IV). In the case where X = OCH_3, three peaks were observed in the visible region with the two higher energy bands being of equal intensity. In all cases, the lower energy band was the strongest (e.g., $Cp_2Ti(S\text{-}p\text{-}C_6H_4OCH_3)_2$ in THF solution, ϵ = 4770 M^{-1} cm^{-1} (546 nm), 3470 M^{-1} cm^{-1} (420 and 386 nm)). The ϵ values are in close agreement with those presented for the d^0 niobium analogue $[Cp_2Nb(S\text{-}p\text{-}C_6H_4OCH_3)_2][BF_4]$, where ϵ = 4500 M^{-1} cm^{-1} (550 nm) and 2100 M^{-1} cm^{-1} (456 nm).[2] As the electron-donating ability of X increased, the transitions in the visible region shifted to lower energies.

An additional strong band at lower energy is observed in the electronic spectra of heterobimetallic complexes $Cp_2Ti(\mu\text{-}S\text{-}p\text{-}C_6H_4X)_2Mo(CO)_4$. It overlaps with the band at ca. 540 nm to form an ill-defined broad envelope. This new band is believed to be due to a charge-transfer transition involving both metal centers.[1i] The higher energy components of the spectrum are practically unchanged as compared with those of $Cp_2Ti(S\text{-}p\text{-}C_6H_4X)_2$ (Table IV), the feature also observed by Braterman et al.[1i,j]

Infrared Data. The solution ν(CO) spectra for the $Mo(CO)_4$ moiety in the titanium bimetallics were consistent with a cis-disubstituted complex of C_{2v} symmetry with the three strongest bands overlapping each other. Individual band positions (Table IV) are the same within the resolution of the instrument indicating that the $Mo(CO)_4$ unit is largely unresponsive to the electronic differences in the thiolate ligand as far as the IR probe is concerned. In fact the ν(CO) IR values of $Cp_2Ti(\mu\text{-}SMe)_2Mo(CO)_4$ are very similar to those of this series.[1i,j]

Kinetics of $Cp_2Ti(S\text{-}p\text{-}C_6H_4X)_2$ Displacement by CO from $Cp_2Ti(\mu\text{-}S\text{-}p\text{-}C_6H_4X)_2Mo(CO)_4$ (X = OCH_3, Cl). The displacement of $Cp_2Ti(S\text{-}p\text{-}C_6H_4X)_2$ from $Cp_2Ti(\mu\text{-}S\text{-}p\text{-}C_6H_4X)_2Mo(CO)_4$ (X = OCH_3, Cl) by CO was monitored by the disappearance of the ν(CO) stretching frequency at 1909 cm^{-1} for X = OCH_3 or 1913 cm^{-1} for X = Cl. Since polar coordinating solvents have been shown to promote disruption of the bimetallics, vide supra, the reaction was performed in toluene to circumvent solvent-assisted pathways in the mechanism. Reaction rates were found to be independent of CO concentration above 300 psi.[21] Plots of ln (Abs_t − Abs_∞) vs time were linear over 3 half-lives (Figure 5), and first-order rate constants were calculated from the slopes. The activation parameters, calculated from Eyring plots (Figure 6), are given in Table V. The positive values of $\Delta S^{\ddagger}$ were attributed to increased disorder due to loss of the chelating

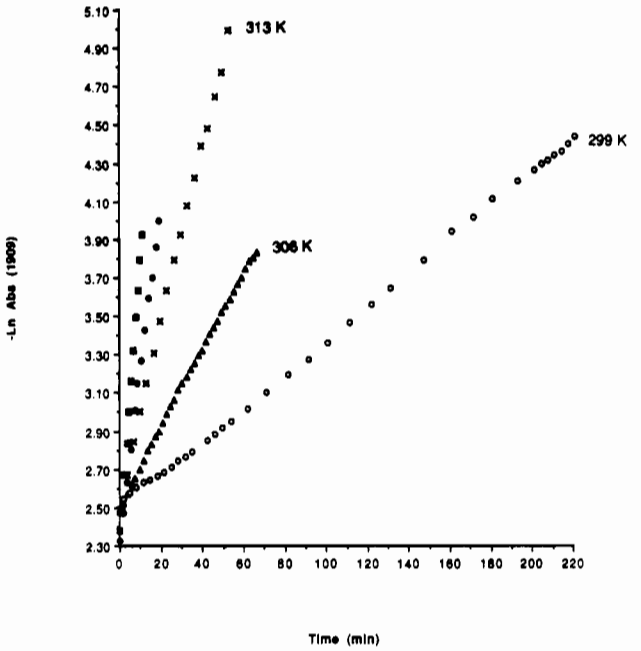

Figure 5. Plot of −ln Abs vs time for the reaction of CO (500 psi) with $Cp_2Ti(\mu\text{-}S\text{-}p\text{-}C_6H_4OCH_3)_2Mo(CO)_4$ in toluene (1909-cm^{-1} band): ●, 318 K; ⊡, 323 K.

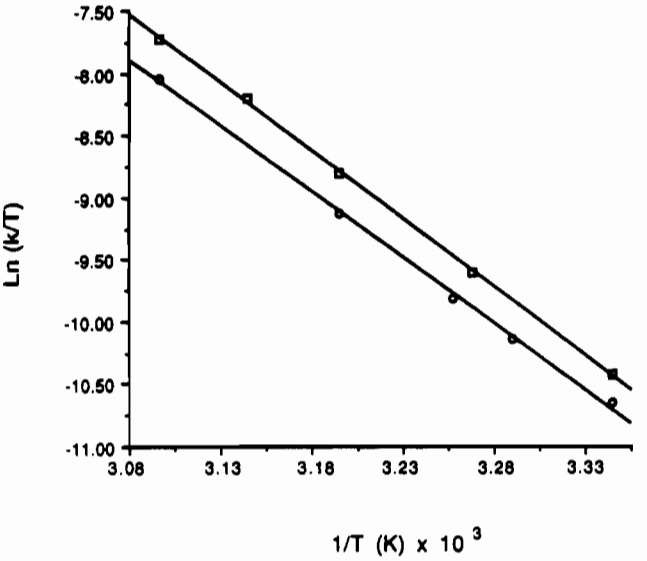

Figure 6. Eyring plot for the reaction of $Cp_2Ti(\mu\text{-}S\text{-}p\text{-}C_6H_4X)_2Mo(CO)_4$ with CO at 500 psi in toluene: □, X = OCH_3; ○, X = Cl.

Scheme III

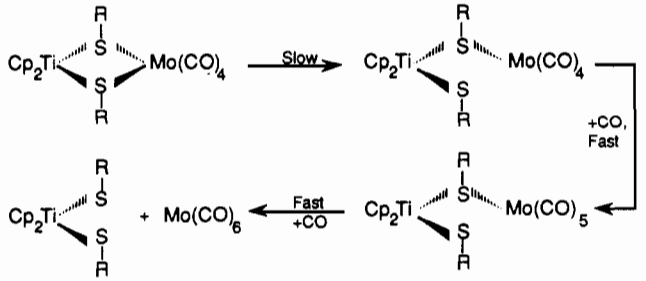

effect when the metallocene–thiolate ligand became monodentate according to the proposed reaction mechanism in Scheme III. Note that Scheme III suggests $Cp_2Ti(SAr)_2$ as a primary product, as it is when the displacing ligand is triphenylphosphine. With CO, however, a subsequent reaction of the bent metallocene over long reaction times gives an unknown product. The rate-determining step in the reaction of CO and the bimetallic is the one involving dissociation of the thiolate group from the $Mo(CO)_4$ fragment followed by rapid CO substitution in the open coordination site. In another fast step the remaining thiolate group is lost and replaced by CO to form $Mo(CO)_6$.

It is instructive to compare the activation data for the CO disruption of the heterobimetallic complexes studied here to the data obtained for substitution of 2,5-dithiahexane (DTH) by phosphites in $(DTH)M(CO)_4$ (M = Cr, Mo).[23] While the substitution mechanism for the Mo compound was determined to be an associative process with negative $\Delta S^{\ddagger}$ values, −78.7 to −85.8 J/(mol·K), the Cr analogue was found to react through a dissociative process with $\Delta S^{\ddagger}$ values of 1–34 J/(mol·K). Similar small and positive values are found here for the Ti–Mo heterobimetallic complexes. The $\Delta H^{\ddagger}$ values, 99.5–109.5 kJ/mol, for the Cr complex are in good agreement with the values obtained for the heterobimetallic complexes reported herein. The $\Delta H^{\ddagger}$ values for the Mo complex, 66.5–68.2 kJ/mol, are smaller due to a bond-making process coinciding with a bond-breaking process.

Concluding Remarks

A two-pronged examination of the stereochemical nonrigidity in heterobimetallic complexes containing the bent metallocene–thiolate fragment has been carried out. Kinetic measurements of CO displacement of the metallocene–thiolate ligand have yielded an estimate of the Mo–S bond strength of ca. 86 kJ/mol for the complexes $Cp_2Ti(\mu\text{-}S\text{-}p\text{-}C_6H_4X)_2Mo(CO)_4$ (X = OCH_3, Cl). This value is on the order of ~30 kJ/mol larger than the free energy of activation calculated from VT ^1H NMR data for the fluxional process. The difference is interpreted as evidence that the CO-substitution reaction and the site-exchange phenomenon have different rate-determining steps. Thus, of the two mechanisms presented earlier (Schemes I and II) which serve to interconvert the heterobimetallic endo(anti) and endo(syn) conformations, we conclude that the bond-breaking mechanism is not consistent with the data, leaving the pyramidal inversion at sulfur as a more reasonable reaction pathway.

The substituent effects (i.e., the nature of X in S-p-C_6H_4X) on $\Delta G^{\ddagger}$ for the CO-substitution reaction are nil, and substituent effects on the $\Delta G^{\ddagger}$ for the fluxionality process are probably also insignificant. In addition, the CO stretching frequencies in the infrared spectra of the $Mo(CO)_4$ fragment show little or no dependence as the substituents are varied, either in this series of para-substituted S-aryls or between S-aryl and S-alkyls! In view of the fact that the bonding in the MS_2M' core of these d^0–d^6 heterometallics has been described as containing at least some "back-donation" of the electron density from the electron-rich metal's t_{2g} into the available a_{1g} orbital of the d^0 metal,[1i,24] it is tempting to ascribe this insensitivity to compensating factors such as S donor ability and Mo→Ti dative bonding. Caution in this regard must be taken, however, since there is a body of literature which shows the $Mo(CO)_4$ fragment of $RSCH_2CH_2SRMo(CO)_4$ to also be insensitive (as far as ν(CO) is concerned) to a variety of substituents on sulfur, i.e., in a situation where clearly no Mo→M dative bonding is possible.[1j,k,5a] In contrast, the redox potentials show a pronounced substituent effect on a Ti-based reduction.

$\Delta G^{\ddagger}$ for the fluxionality in $Cp_2Ti(\mu\text{-}S\text{-}p\text{-}C_6H_4X)_2Mo(CO)_4$ (~50 kJ/mol) is significantly smaller than was reported for the $[Cp_2Ti(\mu\text{-}SEt)_2CuPR_3]^+$ heterobimetallic (~72 kJ/mol).[1o] This is reasonable upon consideration of the more tightly bound TiS_2M' core in the case of the copper derivative. That is, whereas the Ti–S bond lengths are essentially the same in $[Cp_2Ti(\mu\text{-}SEt)_2CuPR_3][PF_6]$ (R = c-C_6H_{11}, 2.47 Å) and $Cp_2Ti(\mu\text{-}S\text{-}p\text{-}C_6H_4Cl)_2Mo(CO)_4$ (2.48 Å), the S–Cu bond distance is 2.24 Å and the S–Mo distance is some 0.3 Å longer, 2.54 Å. The difference may be attributed both to the enhanced thiophilic character of late transition metals as compared to those in the middle of the series, as well as greater steric repulsions in the case of $Mo(CO)_4$ as compared to $CuP(c\text{-}C_6H_{11})_3$. The bulk of the large cyclohexyl substituents is an atom removed from the immediate coordination sphere of Cu whereas the cis-CO groups on $Mo(CO)_4$ are effectively more crowding to the μ-SR ligands. Increased steric interactions are known to lower $\Delta G^{\ddagger}$ values for pyramidal inversion.[5a]

The crystal structures of $Cp_2Ti(\mu\text{-}S\text{-}p\text{-}C_6H_4Cl)_2Mo(CO)_4$ and other such heterobimetallic complexes show the conformation of the mononuclear bent metallocene–thiolate fragment to be by and large retained upon coordination to the $M'L_n$ fragment. That is, the simplistic view of a tetrahedral, sp^3, sulfur with lone-pair orientation set by the presence or absence of π bonding to the bent metallocene (Figure 1) works admirably well in the prediction of stereochemistry of the bimetallics. (More realistic electronic descriptions are available.[1f]) One might expect that there exist combinations of metals with equally strong structure-directing abilities. Whether such metals would be capable of μ-SR bimetallic complex formation, what compromise in structure would be required, and whether redox properties would be grossly affected by such compromised stereochemistries are interesting and open questions.

Acknowledgment. Financial support from the National Science Foundation (Grant CHE 86-03664) is gratefully acknowledged. The R3m/V single-crystal X-ray diffractometer and crystallographic computing system in the Crystal and Molecular Structures Laboratory at the Department of Chemistry, Texas A&M University, was purchased from funds provided by the National Science Foundation (Grant CHE-8513273). We wish to thank Prof. M. Newcomb and Dr. J. H. Horner for help with the DNMR program.

Supplementary Material Available: Tables of atomic coordinates, bond lengths, bond angles, anisotropic displacement parameters, and H-atom coordinates and figures showing a thermal ellipsoid plot (50% probability) and packing diagrams (11 pages); a table of observed and calculated structure factors (17 pages). Ordering information is given on any current masthead page.

(23) Faber, G. C.; Dobson, G. R. *Inorg. Chem.* **1968**, *7*, 584.
(24) Rousseau, R.; Stephan, D. W. *Organometallics* **1991**, *10*, 3399.